PETROPHYSICS, VOL. 59, NO. 3 (JUNE 2018); PAGES 276–287. DOI: 10.30632/PJV59N3-2018t1

TUTORIAL

What is It About Shaly Sands? Shaly Sand Tutorial No. 3 of 3

E. C. Thomas

Editor's comment: This article is part of a series of short "tutorial-like" notes styled to mentor users of digital well logs in becoming confident practitioners of petrophysics.

At the close of Shaly-Sand Tutorial Part 2, I implied, or sort-of promised that this final part would provide some guidance or at least guidelines on the application of my favorite models (equations, transforms, or any of your personal preference names) used to calculate water saturation from a combination of electrical conductivity (i.e., inverse of resistivity), total porosity, formation water salinity, fitting parameters based on rock types (m^*, n^*), and of course, formation temperature. I need not remind you that all of these properties/parameters listed above can and do vary rapidly with depth (vertically) and transversely (horizontally) across a given reservoir.

I once requested a second core in a large reservoir which was turned down by the Division Engineering Manager using the following reason: "Easy, I am really doing you a favor because if the second core and its analyses are different than the first, you will spend a lot of time understanding the differences, and I know you will be back with a request for a third core to help in this investigation." This fellow turned a deaf ear to all arguments that I fully expected that each core *would be* different and only through such sorts of studies could we ever improve our ability to predict recovery efficiency and sweep. "Anyway, that's not the job assignment of a petrophysical engineer. Leave that job to the experts." To me it was obvious that this manager *did not know that he did not know* the influence that geology and petrophysics played in selecting the correct earth model to simulate with mathematical models.

Before we delve into double-layer theory and electrical conductivity, I have one more anecdote; this one has a better outcome. One early morning, a friend and colleague sauntered into my office and asked if I had time to answer a question that had been bothering him. He asked so nicely, I could hardly refuse to at least try to help him. By the way, this fellow was a drilling engineer and his problem involved prediction of overpressure magnitude. He stated it thusly, and I paraphrase "I understand the mechanism of undercompaction due to rapid burial by a big river with a big sediment load coupled with extremely low permeability of thick shales. I even understand the lengthy shale compaction experiments of Waxman and Chow at BRC (Shell Bellaire Research Center) and the resulting equations derived therefrom. But all my model runs using the best and newest data do not predict values as high as we see. Is there another mechanism to generate overpressure?" Somehow this smart guy had stumbled into the office of the right petrophysicist and indeed I could help him, but would need more time than his coffee break. A short version of the answer follows.

Just as in Shaly Sand Tutorial Part 2, I request that you refer to Fig. 8 from Shaly Sand Tutorial Part 1 (Fig. 1 in this piece) during this discussion.

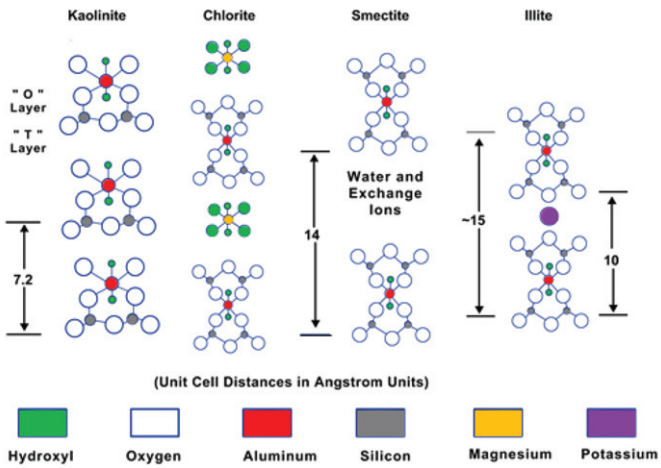

Fig. 1—Reprint of Fig. 8 from Part 1 of this Shaly Sand tutorial. The chemical structures of the "Big Four" clay mineral species using Grim's (1968) notation. Left to right: kaolinite, chlorite, smectite, and illite. The legend shows the correspondence between color and atomic species (courtesy Petroskills).

Remember that the cause of the largest fraction of overpressure is due to undercompaction of sands surrounded by thick shales that reduce the permeability of any escaping brine to such a low value that the pressure in the sands rise as the pore fluids start to carry part of the overburden. There are two additional sources that can lead to a rise in pore pressure. Both are due to shale diagenesis, or more correctly, clay-mineral diagenesis that releases water during diagenetic change. We briefly hinted at this phenomenon in Part 2, near the end of the article. The first diagenetic change affects smectite clay minerals and is enabled by potassium feldspar dissolution and increased temperature with burial depth. The second diagenetic process affects kaolinite clay minerals and is enabled by increased temperature and potassium feldspar dissolution. Chlorite and illite clay minerals are stable in most hydrocarbon producing basins and play no

part in providing extra overpressure. So let's discuss these two diagenetic processes.

Please look at Fig. 8 for smectite and notice the interlayer water and exchange ions (and their six water molecules each) between the repeating units. Compare this part of the bulk volume of the smectite crystal to the same location in the picture of illite. The interlayer space has disappeared! All the brine and hydrated exchange ions have been pushed into the pore space and are replaced by a naked potassium ion and no water. Recall the silica layers above and below the potassium ion have a "hole" in their hexagonal structure, and a hemisphere of potassium fits this space perfectly. The process of potassium entering and exchange ions leaving is explained using quantum mechanics: after all we are dealing with atoms and atomic reactions. The available thermal energy below a depth of ~5,000 ft provides sufficient kinetic energy such that the normally allowed quantized energy levels for each of the clay minerals at room temperature that are degenerate, now split and allow the wave functions of each clay mineral to overlap (recall that at the atomic level and subatomic level ions can exist, simultaneously, as a wave or a particle.) The overlap of the two entities sets the stage for the potassium ion to tunnel in and the interlayer fluid and ions to tunnel out simultaneously without passing through the crystal walls of either clay mineral. Atoms, ions and electromagnetic waves behave under a very different set of rules than the world of matter we exist in. This process is random but as the temperature increases with depth, the process occurs more often due to an increase in kinetic energy, and more potassium ions are available from dissolution of potassium feldspars. During the change, the crystals are called mixed layer clays, favoring smectite at shallow depths before finally becoming all illite at depths ≥20,000 ft. The result is that we find little smectite in Paleozoic formations. That explains the first source of extra fluid in the pore space. The second process is much more complex and involves many steps. Rather than bore you with details, we can state the end results. Kaolinite, a two-layer clay mineral, in the presence of sufficient potassium ions and increased temperature with increase in burial depth and hence time, diagenetically changes into illite, a three-layer clay mineral, losing water and silica in the process. This water is now in the pore space rather than in the crystal—again, a small addition to the pore pressure. The excreted silica is the source of silica cement in some sandstone reservoirs.

Clay-mineral effects aside, "now is the time to talk of many things, the walrus said," and it is time to discuss applications invented for interpretation of shaly sands. We shall skip talking about cabbages and kings. But one more important concept must be discussed again as we did in the very first part of this tutorial. Because we have shown that the dominant mode of deposition of shale is as laminated beds of sand with intermixed shale beds of varying thickness. In these environments it is my recommendation that we do not use incremental processing, rather, we must zone our logs and work with average readings across zones. Please do the research yourself and go look at core slabs, core-slab photos and borehole image logs. Shale laminations of <1-in. to < 1-ft thickness are common. With laminations in this thickness range, attempting to tie a 6-in. digi (digital sampling point) across gamma-ray, density, neutron, sonic, NMR, and electric logs is a futile exercise considering the stick-slip motion of the logs and the various horizontal and vertical response zones. I recommend zoning the logs into plausible beds and computing an average value of the tool response for that bed. Part of the process will be calculating the net-to-gross of the bed so the result will be more representative of the area around the borehole than using incremental readings computed all the way to porosity and water saturation for each 6-in. digi and using cutoffs in these two parameters to count net-to-gross in beds defined later. So when we get to the section on the use of the Thomas-Stieber method, please note: the method was designed for bed averages, not incremental processing. Programmers took my equations and wrote programs for incremental processing without consulting me. The resulting crossplots are largely noise for the reasons stated above and in previous tutorials. Let the user beware.

SHALY SAND MODELS

The logical starting point for discussion of models is an iconic summary of the state-of-the-art of knowledge concerning shaly sands published by SPWLA as a reprint volume in 1982. While this reprint volume is no longer available in printed form, I know many copies are available in oil company, service company and university libraries. Of course there are countless copies in the personal libraries of SPWLA members. My point is that one can find the volume if one tries hard enough. It is my personal belief that any serious student of shaly sands should read the volume in its entirety. It contains not only the previously published work of the leaders in the struggle to understand the properties of shaly sands as well as their log responses in the search to develop quantitative interpretation methods using hand-held calculators and central main-frame computers accessed by punch card decks and 9-track reel-to-reel tape decks at the computer center, but also the temeritous and candid opinions of each of the five reprint volume section leaders that are published nowhere else. Some are profound and some not so much and some ring true today with clear and strong

direction. I will quote some of those that I feel were and are profound during subsequent discussions. The authors of this reprint volume settled on two subsets of models: (1) V_{sh} based and (2) CEC-based, so I choose to use them as well. However, the subset of anisotropic models was not broached by the reprint authors, but I will delve into this topic albeit at a very elementary level.

V_{sh} Models

The earliest attempts to make shaliness corrections to formation evaluation methods settled on using the bulk volume of shale as the correction method. It was simple to apply using the gamma-ray response assuming that only the shale fraction contributed to the gamma-ray response in a shaly sand. This approach had to be modified when one noticed that "clean" sands did not read zero API units. Thus the calculation had to be normalized using the reading in a "clean" sand and a reading in a "pure" shale. As long as the difference in the gamma-ray values was sufficiently different to give acceptable errors, the method gained acceptance. Common values for a clean sand were 20 API units and for a shale, 100 API units, providing 80 API units separation to compute a value of V_{sh} in the shaly sand in question. This method is widely accepted as "The Way" to determine V_{sh} from logs. In the previous two parts of this tutorial on Shaly Sands we have thoroughly discussed why using just a gamma-ray log yields dubious results. In addition to the difficulties discussed previously, early on, other difficulties arose when in two oil provinces the gamma ray could not reliably distinguish between shaly sands and shales. The first example arose in the North Sea fields because of the presence of radioactive mica in the sands, leading to a much-reduced spread in gamma-ray response in the sands and shales. The second example arose in offshore Nigeria where abundant radioactive potassium feldspars in the sands again made discrimination between sands and shales based on gamma-ray response unreliable. Clearly, a different approach was needed and in both environments additional log responses were added to obtain satisfactory discrimination, and many schemes using multiple logs were developed and are in use worldwide to handle radioactive sands. Of course, these methods suffer most of the shortcomings discussed for use of the gamma-ray alone. Workers in shaly sands soon realized the difference between shale and clay minerals and that it was the clay-mineral component that was the cause of shaly sand effects and the gamma-ray log also sensed other radioactive minerals as well and could not be relied upon as a measure of V_{clay}. George Coates, the author of the introduction to the V_{sh} Methods chapter of the Shaly Sand Reprint Volume succinctly stated that "Recognizing that the clay minerals presence perturbed the resistivity measurements as a consequence of the cation exchange capacity of the clay (sic) doomed the V_{sh} models." Please note how profound George was in confining the mistake to use V_{sh} in saturation models only and leaving the door open for correct uses of V_{sh} in geometric applications, such as computing the sand fraction of a given bed. It has been 36 years since George gave us the direction to use in saturation determination, yet even today, throughout the world, practitioners are dutifully using 1970s V_{sh} methods for saturation calculations in shaly sands. How sad!

Cation Exchange Capacity Methods

This section is not intended to be a critical review. I was given the charge to document my knowledge and experience in each tutorial, thus the summary below may be somewhat longer than the reader might have expected. In the previous two parts of the shaly sand tutorial we covered much of the basic chemistry of the generation of charge defects in the bulk lattice of clay minerals resulting in the attraction of hydrated sodium cations from the bulk brine phase. These hydrated sodium cations do not form chemical bonds with the surface of clay minerals but instead form a continuous and variable concentration between bulk concentrations of the brine and an ephemeral contact with the surface. Some years ago, in a personal communication, Pat Worthington of Chevron Research shared with me the results of a study of the contact time of the hydrated sodium cation on the clay mineral surface to be in the range of 1 msec at ambient conditions before being replaced with another hydrated sodium cation. Such a constant exchange is driven by translational motion of the ions and molecules due to their kinetic energy fueled by the thermal bath in which the reservoir rocks reside. One may consider this to be a diffusion gradient or simply a concentration gradient. There is no "bound" water layer that can be captured and measured, unless you consider <1 msec as being "bound" and I do not. Such hydrated cations are also in competition for space on the clay-mineral surface from capillary-attracted water, i.e., hydrogen bonds with the clay-mineral surface, which are van der Waals attraction at a much closer distance to the surface. This competition is fiercer than one might expect, given that each free-water molecule is hydrogen bonded to four adjacent water molecules in a tetrahedral complex. Such a tetrahedral attraction is manifest as surface tension in the porous network. Finally, one has to consider that if the cations are attracted to the negatively charged surface of clay minerals, then the negatively charged hydrated anions are repelled by the same charge field, resulting in an inverse concentration gradient of hydrated chloride anions. The concept of concentration gradients, which was published by Winsauer and McCardell (1953) of Humble Research, is

included in the Shaly Sand Reprint Volume. I have included Fig. 2 from Winsauer and McCardell (1953), which was constructed from thermodynamic calculations.

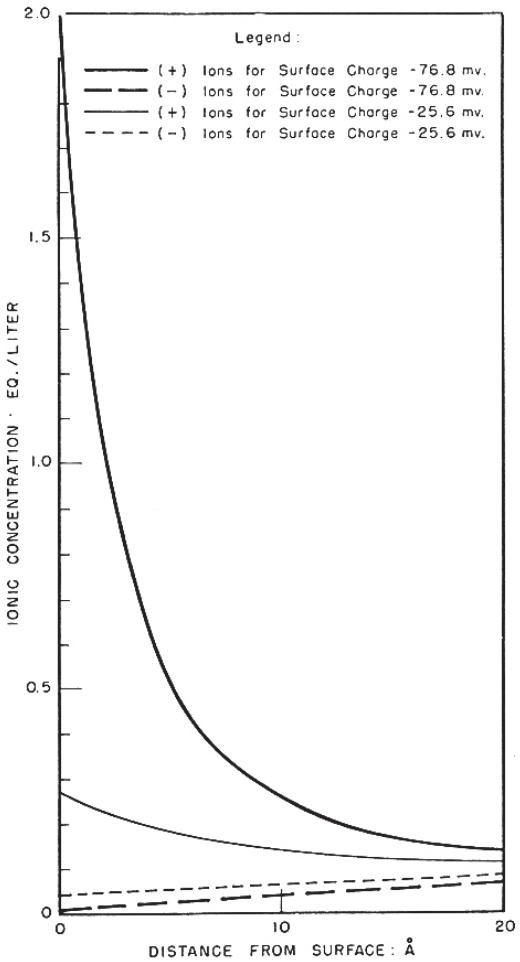

FIG. 2 — DISTRIBUTION OF IONS IN ELECTRICAL DOUBLE LAYER FOR 0.1 N EQUILIBRIUM SOLUTION.

Fig. 2—Distribution of ions in electrical double Layer for 0.1-N equilibrium solution (Winsauer and McCardell, 1953).

Now I ask the reader: Where do you place the boundary for the "bound" layer? Previous authors used a simple geometrical model that placed the six waters of hydration in a plane surrounding the sodium ion. Quantum mechanical considerations require the six water molecules to be in an octahedral complex form and the sodium-to-water distance should have a temperature effect. While the data presented by Winsauer and McCardell (1953) are a source to compute the excess conductivity, they made one poor assumption in the process of computing excess conductivity from their data on shales: They assumed that the geometry of clay minerals does not change with salinity. We now know that smectites swell as the salinity decreases, thus for any shaly sand with smectite or mixed-layer clay minerals the Winsauer-McCardell method is in error. Regardless of the difficulties discussed above, I hope I have convinced you that hydrated sodium exchange ions should not be considered as "bound" water because these hydrated ions are in constant motion due to their kinetic energy from the thermal bath.

Now we switch to a short discussion of the Waxman-Smits equations. One can quickly see what importance Shell placed on understanding the shaly sand effects on calculated water saturation because they paid for two independent rock-based empirical studies, one by Lambert Smits at KSEPL in Rijswijk, The Netherlands, while Monroe Waxman toiled away at EPRC in Houston, USA. When Gus Archie hired Monroe he purposely chose a physical chemist to attack the problem, not a petroleum engineer. The existing techniques Shell was using were cumbersome and slow. Gus felt the approach was a dead end and let Monroe have the freedom to use any method, just as long as the parameters in the resulting equations could be independently determined in the laboratory. Additionally, Gus felt that to keep the result simple so it would be readily used in fieldwork, hence he restricted Monroe to add no more than one additional parameter to Archie's saturation equation, at least for the first approach. Monroe looked at the existing dataset of Hill and Milburn (1956) that consisted of several thousand resistivity measurements on 100% water-bearing shaly sands. Their result was an exponential equation with a logarithm in the exponent. That, my friends, was a beast to solve with only a slide rule in the field. Additionally, the fit required a variable labeled "*b*", but they really had little idea what the parameter was, other than it had some measure of shaliness. Later, the work of Roy Coles in the laboratory identified "*b*" to be the cation exchange capacity per unit pore volume. In keeping with conventions at the time, and since, it was a volume concentration of charged sites, the term Q_v was chosen. This work of Coles ran in parallel with what Monroe was doing. Monroe then had a flash of insight that led him to convert all the resistivity data into conductivity. That change paid off big time, because the exponential fits of Hill and Milburn converted into a linear equation over a wide range of salinities in conductivity space. When water-bearing shaly sands isothermal data are plotted with core electrical conductivity, C_0, on the y-axis and saturating-water conductivity, C_w, on the *x*-axis, all of the data of Hill and Milburn looked similar. Thus we have the type curve shown in Fig. 3.

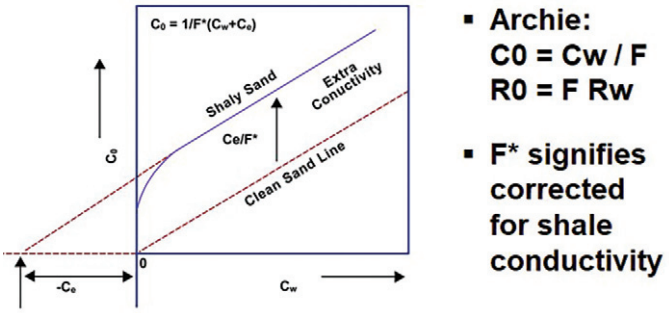

Fig. 3—Example of a C_0-C_w plot for a given shaly sand core plug. For comparison, a similar clean-sand core plug is shown as a dotted line. Note: The clean sand example is generated by deactivating all the exchange capacity sites of the shaly sand core plug thereby allowing both samples to have identical pore geometries and hence plot with identical slopes, *1/F** (courtesy of Petroskills).

As shown in Fig. 3, the data fell into two ranges. For low-salinity data, i.e., low electrical conductivity, the response was exponential. However, from seawater conductivity and above, the response was linear. Let us examine the linear portion first. We observe that when we extrapolate the linear portion to a value of $C_0 = 0$, the line does not go through the origin, but has a positive y-intercept when $C_w = 0$ and a negative x-intercept when $C_0 = 0$ and the linear equation has a slope = t , later defined as $1/F^*$.

Let us now write the clean sand water-bearing Archie's equation in conductivity space:

$$C_0 = \frac{1}{F} C_W \quad , \tag{1}$$

where the slope is $1/F$.

It becomes quickly apparent that this equation does not work, as it requires the line to go through the origin. However, if we modify the equation to account for the extra electrical conductivity, we can write a shaly sand Archie-like equation as

$$C_0 = \frac{1}{F^*}\left(C_W + C_{XTRA}\right) \tag{2}$$

where C_{XTRA} is the extra electrical conductivity.

Now we observe when $C_w = 0$ the y-axis intercept is C_{XTRA}/F^* and when $C_0 = 0$ and the x-axis intercept is $-C_{XTRA}$. The parameter $1/F^*$ is used to designate this quantity as a shaly sand formation factor that accounts for the extra electrical conductivity. Because we are applying $1/F^*$ equally to C_w and C_{XTRA}, it implies that the two terms are the components of a parallel electrical circuit. In such a formulation, the clay-mineral hydrated cations are allowed to roam about the pore and are not confined to some "bound" layer of differing salinity and conductivity as the interstitial brine. This unlimited diffusion model conforms to the concentration gradients shown in Fig. 2.

Now we wish to bring some quantification between C_{XTRA} and shaliness. We do this by breaking conductivity into two parts, a volume concentration term and an equivalent conductance (standard physical chemical formulation). For the linear portion of the response, the equivalent conductance term is at its maximum value and constant leading to a linear relationship. We shall designate the letter B to denote the equivalent conductance of the hydrated sodium cations. The volume concentration term is our old friend, Q_v, the cation exchange capacity per unit pore volume. Thus we can write

$$C_{XTRA} = B_{MAX} Q_v , \tag{3}$$

where the units of Q_v are equivalents/liter or meq/ml or meq/cm^3 and the units of B are mho-cm^2/meq and the product of these two terms is conductivity, with units of mho/cm. In the core laboratory we make three measurements of C_0 at concentration values of 100-, 150-, and 200 kppm Na^+Cl^-. With proper laboratory procedures, one may routinely determine $B_{max}Q_v$ with an R^2=0.9999**.** Please note that this measurement should always be made at reservoir temperature as brine and clay-mineral counterions have differing temperature coefficients.

Now we can turn our attention to the fresh end of the C_0-C_w plot, which is exponential. Two interesting facts: If we extrapolate to $C_w = 0$, C_w does not go to zero for wet samples. So even with no brine ions, the hydrated exchange cations can still carry current by jumping from one exchange site to the next. However, if we dry the core, it has no innate conductivity. This proves that water plays a crucial role in the conductivity of shaly sands. Then after obtaining $B_{max}Q_v$, one can back up to the correct value of C_w (known freshwater value) in the nonlinear portion of the curve at reservoir T and obtain a value C_0 at reservoir C_w. Apply the same $1/F^*$ you determined from the previous measurement, extrapolate back to $C_0 = 0$ and obtain a new value of BQ_v for the freshwater reservoir. That is all you need to do since the terms B and Q_v are always used as a product in the Waxman-Smits equations. Also once we have F^* from a C_0-C_w plot, we can use

$$F^* = \phi_T^{-m^*}, \tag{4}$$

Where ϕ_T is total porosity (i.e., density log porosity or Dean-Stark core porosity) and F^* and m^* state that the measurement has shale effects included and corrected for.

Lastly, Monroe extended the 100% water-bearing equations to account for the presence of hydrocarbons. The method chosen by Monroe was to use the same concept as

relative permeability, where the permeability of a given phase is proportional to its saturation, i.e., oil relative permeability goes as the oil saturation.

Thus Monroe reasoned that as the fraction of water decreases, the contribution of the clay-mineral counter ions becomes a larger part of the parallel circuit as the fraction of the brine conductivity decreases. Consequently, the hydrocarbon-bearing effective brine conductivity increases as the water saturation decreases. Therefore, as one goes up in the oil column the shaliness correction increases.

Monroe expressed the equation as

$$Q_V^* = \frac{Q_V}{S_W} \ , \tag{5}$$

which leads to the saturation equation

$$I = \frac{C_0}{C_t} = S_W^{-n^*} \left(\frac{C_W + BQ_V}{C_W + BQ_V^*} \right) \ . \tag{6}$$

This equation is straightforward and can be easily implemented in Excel.

The main drawback to Eq. 6 is that it applies to the homogeneous dispersed clay-mineral case, and should not be used in laminated shaly sands without first preprocessing with the Thomas-Stieber equation to remove the effects of the laminations. The Waxman-Smits equation works well for the remaining sand fraction. Of course, without core it is difficult to pin down BQ_v. But when you are fortunate enough to encounter a large water leg, then one can use the Thomas-Haley method (Thomas and Haley, 1977) to estimate BQ_v at reservoir conditions of temperature and salinity. Read on.

LAMINATED, STRUCTURAL, AND DISPERSED SHALE DIFFERENTIATION

A novice in this field may still not appreciate just why continuing the use of their corporate directive V_{sh} model, e.g., the Indonesia Equation, is error prone but I have always felt that a simple, thorough example that demonstrates the range of the overlooked consequences makes one a believer. Thus, we use a simple model as a pedagogical device to show that the addition of shaliness in the three different distributions in the title of this section, one ends up with different values of total and effective porosity. The modeling exercise begins with a clean sand with a fixed value of total porosity, ϕ, and the model will hold its bulk volume constant for the exercise. We use the following nomenclature: X is the bulk volume fraction, ϕ is the pore volume fraction of bulk volume and called porosity, $(1 - \phi)$ is the grain volume fraction of the bulk volume, and GR is the gamma ray tool response in API units. The following subscripts are used: *sd* is sand, *sdgr* is sand grains, *sh* is shale, *shgr* is shale grains, *cl* is clean sand, *disp* is dispersed shale in an otherwise clean sand, *str* is structural shale in an otherwise clean sand, and *lam* is laminated shale in an otherwise clean sand. In our models, the shale has porosity just as it does in nature. However, the pore sizes of the shale are so small that they contain only irreducible water and is thus immobile and not effective for fluid flow.

Structural Case

Initial Conditions: $\phi_{cl} = 0.30$.

The total bulk volume of shale grains we add is $X = 0.15$. To keep a constant bulk volume, we must remove the same volume of clean sand grains. The individual shale grains have their own porosity, $\phi_{sh} = 0.10$ and the resulting equation is

$$\phi_{str} = \phi_{cl} - X_{sd}\,\phi_{sdgr} + X_{sh}\,\phi_{shgr} \ . \tag{7}$$

Because $\phi_{sdgr} = 0$, the equation reduces to

$$\phi_{str} = \phi_{cl} + X_{sh}\,\phi_{shgr}, \tag{8}$$

and if we substitute in the values for our example case one obtains

$$\phi_{str} = 0.30 + 0.15\ 0.1 = 0.315, \tag{9}$$

which shows that the density log reads higher total porosity in the structural shaly sand than it would in the original clean sand case. Many users forget that shales have porosity and would incorrectly consider the movable fluids volume to be larger than its true value. Therefore, for this example $\phi_T = 0.315$ and $\phi_E = 0.30$.

Now, if we write a similar equation for the gamma-ray response, use initial conditions of $GR_{clean} = 20$ API units and $GR_{shale} = 100$ API units, and use similar logic, we can write the response for structural shale as

$$GR_{str} = GR_{cl} - X_{sh}GR_{cl} + X_{sh}GR_{sh}, \tag{10}$$

then, by gathering terms we derive

$$GR_{str} = GR_{cl} + X_{sh}(GR_{sh} - GR_{cl}), \tag{11}$$

and if we substitute back into this equation the initial conditions we arrive at

$$GR_{str} = 20 + 0.15(100{-}20) = 20 + 12 = 32\text{API} \tag{12}$$

Dispersed Case

Using the same initial conditions and same bulk volume

of shale added. The only difference is that the added shale (mostly authigenic clay minerals) just takes up pore space. But now the displaced pore volume is due to the grain volume of the shale only. Hence we can write the equation thusly:

$$\phi_{disp} = \phi_{cl} - X_{sh}(1 - \phi_{sh}). \quad (13)$$

I like to call $(1 - \phi)$ a new term I have coined, "grainosity." I have not had many users to adopt this term, and it sounds so logical. Another Easy Money bust. But if we substitute the same numerical initial conditions used above, we observe that

$$\phi_{disp} = 0.30 - 0.15(0.90) = 0.165 \quad (14)$$

Wow! The same bulk volume shale added as the structural case and we see ϕ_T fall from 0.315 to 0.165. Astounding!

If we use the same logic to write the gamma-ray response for dispersed shale, we obtain

$$GR_{disp} = GR_{cl} + X_{sh}GR_{sh} = 20 + 0.15(100) = 35\text{API}, \quad (15)$$

which is slightly higher than the structural case considered above.

Laminated Case

Using the same initial conditions and same bulk volume of shale added. For this model, in order to add a lamination of shale we must first remove the same bulk volume of clean sand in order to keep the bulk volume constant. The model equation is expressed as

$$\phi_{Iam} = \phi_{cl} - X_{sh}\phi_{sd} + X_{sh}\phi_{sd}. \quad (16)$$

Thus we have three different linear equations that describe the change in porosity for various amounts of shale added. If we use the same logic to write the gamma-ray response for laminated shale, we obtain

$$GR_{Iam} = GR_{cl} - X_{sh}GR_{cl} + X_{sh}GR_{sh}. \quad (17)$$

Let us now compute the resulting values of total porosity and gamma ray response for the model cases. We obtain

$$\phi_{Iam} = 0.30 - 0.15(0.30) + 0.15(0.10) = 0.27. \quad (18)$$

Thus $\phi_T = 0.27$ and $\phi_E = 0.255$.

Similarly,

$$GR_{Iam} = 20 - 0.15\,20 + 0.15\,100 = 20 - 3 + 15 = 32\text{API}. \quad (19)$$

Let us put all these results into a table for handy comparison.

Table 1—Model Results

	Model		
Results	Laminated	Dispersed	Structural
Total porosity (ϕ_T)	0.27	0.165	0.315
Effective porosity (ϕ_E)	0.255	0.15	.3
Gamma-ray response (API units)	32	35	32

Initial values: $\phi_{sd} = 0.30$, $\phi_{sh} = 0.1$; $V_{sh} = 0.15$; $GR_{sd} = 20$ API; $GR_{sh} = 100$ API.

One can easily observe from the table above how large the error might be when using the normalized gamma ray alone to correct the density log for shaliness to arrive at a shale-corrected total porosity without taking the shale distribution into account.

Thomas-Stieber Method: A Simple First-Order Correction for Anisotropy Caused by Shale Laminations

I am sure you that have picked up my thread through these tutorials that the earth is manifestly not homogeneous and it is folly to ignore anisotropy as reality in our approach to formation evaluation. Observations of road cuts, river bank bluffs, canyon walls and the like, as well as slabbed faces of whole cores, give ample proof that we live within a layered environment. It makes no difference as to the process of deposition—wind, water, volcanic, gravity—they all result in depositing layers initially. Some become distorted terribly by enormous earth stresses while some just lay quietly and are squeezed inexorably by more sediments on top. When conditions are correct to allow pore fluids to escape, some sediments are reduced to zero porosity, all the while keeping their laminated structure.

We begin with handling the case when the borehole and the sand-shale laminations are perpendicular and we have no new-fangled tools that can unscramble tilted boreholes with tilted beds and derive horizontal and vertical resistivity values, which allow us to make second-order corrections for anisotropy. Even in this better approach, we still have to approximate the effects of crossbeds in deltaic sediments. But the big unknown will still be the effect of unresolved shale laminations, i.e., shale beds smaller than 1- to 2-ft thickness. These size laminations will hardly be observed on induction logs, but simply will be averaged over its large vertical response. Their presence will be noticed on density logs but will remain unresolved and averaged, just as with the induction log. We can take these beds out of our sand counts, but if we use Thomas-Stieber method we must avoid double dipping, as we will be using averaged values of the density which will include these 1- to 2-ft beds.

By restricting ourselves to a two-component model,

i.e., sands and shales, we can take a deterministic solution approach if we have two independent borehole tools that have approximate similar volumes of investigation. As you expect from the model discussed above, we choose to work with a borehole-compensated density log to determine total porosity when we know the flushed-zone fluid density and average grain density. This tool averages over a ~3-ft vertical interval and a directed wedge away from the borehole wall with a radial depth of response of approximately 12 in. The second borehole device we choose to use is the natural gamma-ray sonde. Its response is roughly spherical and senses gamma radiation from up to 12 in. from the borehole and includes any gamma radiation from the borehole fluids and invading fluids. The latter two sources are usually negligible, except for KCl polymer muds.

In the models shown in the previous section, we emphasized that both the density log and gamma-ray log have linear responses with porosity for a sand-shale environment. The resulting model we developed is shown in Figure 4.

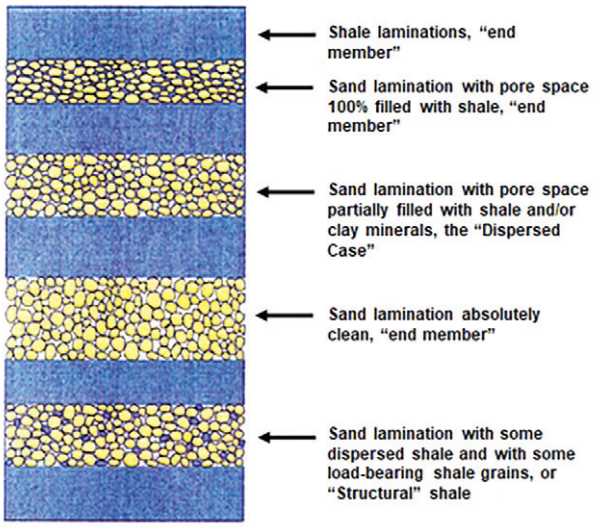

Fig. 4—Sand and shale configurations in the Thomas-Stieber model (courtesy of Petroskills).

Thus, we can solve these previous equations simultaneously for bulk volume fraction of shale and total porosity of the sand fraction as long as we restrict ourselves to only two modes of occurrence of shale. Otherwise we would be trying to solve three sets of equations with only two log responses, which is a no-no. One of the most common cases is when the volumetric concentration of structural shale is less than 10%, thus we choose to solve for a mixture of laminated sand and shale with dispersed shale in the sand laminations. This procedure allows us to then subtract the effects of the shale laminations and obtain the actual porosity of the sand layers. Previously, we only saw the porosity of the mix of shaly sand and shale. But with this approach we remove the effects of the shale laminae, i.e., anisotropy, and obtain the porosity of the shaly sand alone. The simplest way to understand this procedure is by way of a graphical solution. But before we develop the Thomas-Stieber's triangle graphical solution, let us pull together many of the threads of all the previous tutorials.

Step one of an evaluation (after depth matching logs) is to zone the logs over the zone of interest. Most of us never have hydrocarbon zones greater than a few hundred feet, so most of us have gross zones 200 ft with subzones <50-ft thick. But you, as the interpreter, must look at all logs and subdivide into intervals that have similar responses and place bed boundaries at inflection points across all logs. Remember changes at gas/oil and oil/water contacts and to stay in contact with the paleontologist so as not to mix geologic ages in a single evaluation interval. Also you will have to weed out the shale laminations/beds that are thick enough to be partially resolved and keep them out of your sand counts. For each of your zones, take average readings of each log, bearing in mind their response characteristics, particularly shoulder-bed effects. Assign a reference number to each zone and it is this number you will use for the graphical solution. Thus, for your 200-ft bed you will not have to deal with 400 points, as in an incremental evaluation, but rather you will have fewer than 50 and perhaps fewer than 20. Remember that you are dealing with averages over zones >3-ft thick and for induction logs, >12-ft thick.

An example of a naked Thomas-Stieber plot follows. It is for the case where $\phi_{sh} = 0.10$ and $\phi_{sd} = 0.30$.

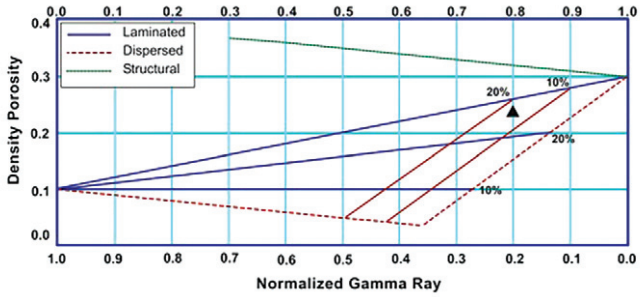

Fig. 5—Example of geometrical solution of the Thomas-Stieber equations for laminated sands and shales with the sands containing dispersed shale. For reference, we show a computed line for only structural shale additions. This figure is constructed having previously deduced clean sand and shale values of porosity and gamma ray.

One begins the plotting exercise with the porosity and gamma ray values for all the zones you feel are the same rock type plotted together. The first step is to select the shale point. You may shift it later. Construct a triangle starting at the shale point and draw a straight line to where you believe the clean-sand point should be based upon your knowledge

of the formation, geologic age, and depth. The clean-sand point must pass a smell test of reasonableness for the area. Once you have selected a clean-sand point, the equations fix the third point of the triangle. David Patrick Murphy has written a freely available macro for Excel that performs this exercise interactively. He asks only that he be cited when one uses it. He wrote his macro to expect incremental data, hence to use the program you will have to construct artificial curves every 6 in. across the averaged zones. The user can move the shale point in both porosity and gamma-ray space as well as the clean-sand point similarly. The third point of the triangle is computed for you. I suggest you move these points around until you have encompassed most all of the higher porosity values, keeping the clean sand point as low as possible. Just remember, there will be no data point to fall at the clean-sand point; after all, we are evaluating shaly sands, whereby not having an actual clean-sand point is to be the usual case.

However, if we retreat a step and look back at Fig. 5, you will observe a single triangular point on the graph to represent a single-zone average. To graphically solve for the sand fraction of the zone, one extrapolates upward with a line parallel to the dispersed line until it intersects the laminated line. This point represents the sand fraction, SF, using a linear construction using 1.0 at the clean-sand point and 0.0 at the shale point. To determine the actual porosity of the shaly sand free of shale laminations, one constructs a line beginning at the shale point and running through the data point and continuing on to intersect the dispersed-model line. One then reads the shaly sand porosity value on the porosity scale on the y-axis. Graphical solutions are slow and cumbersome, so I offer mathematical solutions provided by Arthur Purpich. Because Arthur started with my nomenclature and earliest simplifications of the equations, the following mathematical solutions use an inverse gamma-ray scale where shale is zero and sand is one. This is computed as follows:

$$\gamma = \frac{GR_{sh} - GR_{\log}}{GR_{sh} - GR_{sd}} \quad \gamma_{sh} = 0 \quad \gamma_{sd} = 1. \tag{20}$$

To simplify the equations, we used a parameter ζ defined as

$$\varsigma = \frac{GR_{sh}}{GR_{sh} - GR_{sd}} \ . \tag{21}$$

Using these parameters, the mathematical solution for a laminated sand-shale model containing dispersed shale is given by

$$Sand\ Fraction\,(SF) = \frac{\gamma\left(1-\phi_{sh}\right) - \zeta\left(\phi_T - \phi_{sh}\right)}{\left(1-\phi_{sh}\right) - \zeta\left(\phi_{sd} - \phi_{sh}\right)}$$

Total porosity of the shaly-sand fraction is then

$$\phi_{Tsd} = \phi_{sd} - Z_d(1 - \phi_{sh}), \tag{22}$$

where Z_d is defined as

$$Z_d = \frac{1 - \frac{\gamma}{SF}}{\zeta}, \tag{23}$$

where Z_d is the bulk volume fraction of dispersed shale in the shaly sand. But whoa you say! What is this new unknown parameter and how have we solved for it without violating the two unknowns from two parameters? Well the answer is simple—we have added new known values of shale and sand when we establish the Thomas-Stieber triangle. To understand this, let us look below at Fig. 6.

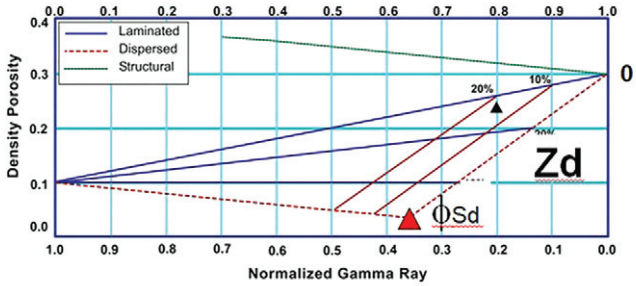

Fig. 6—This is Fig. 5 with the dispersed line rescaled as Z_d. Because we know the value of bulk volume shale in a clean sand is zero, we set the clean-sand point Z_d = 0. Likewise, because we cannot put more dispersed shale into a clean sand than its available pore space, we can set the bottom point of the dispersed line as $Z_d = \phi_{cl}$.

Because we now know the fraction of sand and shale we can use this information to parse the induction log into a shale resistivity and a shaly sand resistivity. Such a situation can be approximated only when the borehole and laminated zone are perpendicular. For small deviations from the latter case we can make corrections if we know the dip. These equations were published by Terry Hagiwara (1988) and independently, by Jim Klein (1991). But if we retreat to the simple perpendicular case, we can write the following equation to parse the induction log:

$$\frac{1}{R_{\log}} = \frac{X_{sh}}{R_{sh}} + \frac{\left(1-X_{sh}\right)}{R_{sd}}, \tag{24}$$

where X_{sh} is the shale fraction (1 − SF).

We solve for R_{sd}, the shale laminae-free value of shaly sand resistivity. This equation assumes that the sand laminae and shale laminae form a parallel circuit. Because this equation has our desired parameter in the denominator,

nature can, and has conspired to configure resistivities such that we try to divide by zero and the algorithm blows up. So as a fall-back approximation, we can put the laminae into a series circuit, shown below, which never blows up.

$$R_{\log} = X_{sh}R_{sh} + (1 - X_{sh})R_{sd}. \tag{25}$$

Consequently, we now have a value of shaly sand resistivity free of shale laminations. This is not a perfect solution by any means, but it does make a first-order correction for the anisotropic effects for the stated conditions. Thus we have a value of resistivity that approximates that of a homogeneous formation! We can use this value of resistivity in the Waxman-Smits equations!

If only we knew what value of BQ_v to use—but wait, the world may not be at an end just yet. If we have a water leg in our zone or a nearby wet (water-bearing) zone of the same rock type, we can work our way out of the dilemma through clever manipulation of a combination of Waxman-Smits and Thomas-Stieber and published as the Thomas-Haley solution for BQ_v (Thomas and Haley, 1977).

Thomas-Haley Solution for BQ_v in Water-Bearing Shaly Sands

We begin with the water-bearing form of the Waxman-Smits equation, given by

$$\frac{R_w}{R_0} = \frac{1}{F^*}\left(1 + R_w B Q_v\right), \tag{25}$$

where all terms have been explained earlier.

The next step is to rearrange this equation into a form we find more convenient, namely,

$$\frac{F^*}{R_0} = \frac{1}{R_w} + BQ_v = C_{wa}, \tag{26}$$

where C_{wa} is defined as the apparent water conductivity. Of course, C_{wa} is the inverse of our old friend, R_{wa}, the apparent water resistivity.

We now make the reasonable assumption that all the cation exchange capacity (*CEC*) arises from the dispersed shale in the sand laminae and that the CEC of a zone will be proportional to the volume of dispersed shale in the sand laminae. We can then write

$$CEC = CV_{disp}, \tag{27}$$

where V_{disp} is the volume of dispersed shale in a zone, liters, and C is the CEC per liter of dispersed shale in eq/L (treat as a constant for a given zone).

We can also express the pore volume of the sand laminae in a zone as

$$PV = \phi_{sd}V_{sd}, \tag{28}$$

where ϕ_{sd} is the total porosity of the sand laminae, and V_{sd} is the volume of sand laminae in a zone in liters.

At this point in the derivation you are probably wondering what gives! How does one determine the actual volume of a zone? Bear with me. It will all work out in the end.

Now recall the definition of Q_v (defined above), $Q_v = CEC/PV$, hence

$$Q_v = \frac{CV_{disp}}{\phi_{sd}V_{sd}} \tag{29}$$

and recall that V_{disp}/V_{sd} is the definition of Z_d from a Thomas-Stieber plot.

Consequently, we can now write

$$Q_v = \frac{CZ_d}{\phi_{sd}}, \tag{30}$$

and we substitute this back into the apparent water conductivity equation, to obtain

$$\frac{F^*}{R_0} = C_{wa} = \frac{1}{R_w} + BC\frac{Z_d}{\phi_{sd}}. \tag{31}$$

By using $F^* = \phi_{sd}^{-m^*}$ and $R_0 = R_{sd}$ we now arrive at

$$C_{wa} = \frac{\phi_{sd}^{-m^*}}{R_{sd}} = \frac{1}{R_w} + BC\frac{Z_d}{\phi_{sd}}, \tag{32}$$

which the water-bearing Waxman-Smits equation.

Then if we combine the Thomas-Stieber data with the parsed resistivity data in the wet zones we can plot C_{wa} vs. Z_d/ϕ_{sd} and the result is a plot like that shown in Fig. 7.

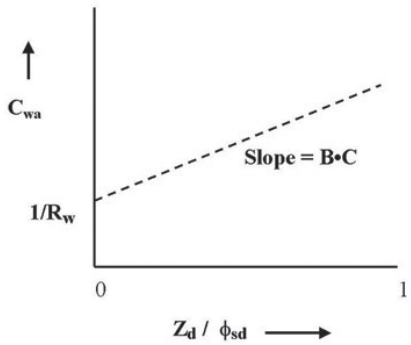

Fig. 7—Plot of C_{wa} vs. Z_d/ϕ_{sd} yielding a straight line with a slope = BC and intercept of $1/R_w$.

Lastly we use the slope of the line to get BQ_v without ever knowing any of the previous terms individually.

$$BQ_v = (BC)\frac{Z_d}{\phi_{sd}}, \tag{33}$$

where BC is the slope of the line in Fig. 7.

We now can compute a value of BQ_v at reservoir conditions which we can map back into our hydrocarbon-bearing zones using the parameter Z_d, which is much more realistic than using either gamma ray or $1/\phi$ as has been done in the past.

Therefore, our quest has come to an end. We have slain Smaug, and the bug-a-boo of not having a tool to get Q_v as an excuse for not using the Waxman-Smits model or even dual-water model in its original configuration, which used Q_v.

ACKNOWLEDGEMENTS

The author is most grateful to the management of PetroSkills, which has permitted the use of their figures, in part, for this tutorial. Additionally, the author is indebted to his colleagues John Stieber, Ron Haley, David Patrick Murphy, Paul Connolly, Mark Shannon, Rich Ostermeier and,of course, Bob Sneider and Monroe Waxman whose wise mentoring and endless discussions have helped me arrive at a position where I could pen this tutorial. The actual list of colleagues that have helped me along the way is much too long for this acknowledgement and I regret not being able to give them a thank you in print. Lastly, but certainly not the least, I would be remiss if I did not express my profound gratitude for the guidance and superior editing skill provided by Stephen Prensky and Carlos-Torres-Verdin to whip my tutorials into useful articles of real help for the novice petrophysicist.

NOMENCLATURE

Symbols

b = Hill-Milburn shaliness parameter
B = equivalent conductance of the sodium exchange ion
B_{MAX} = the maximum value exhibited for a given shaly sand sample at a given temperature
CEC = cation exchange capacity
C_{XRTA} = extra electrical conductivity
C_w = saturating water conductivity
C_{wa} = apparent water conductivity seen in a shaly sand
C_0 = core electrical conductivity
F = Archie's formation factor
F^* = Waxman's formation factor for a shaly sand indicting it has shaliness effects included
GR = gamma ray, API units
Q_v = cation exchange capacity per unit pore volume
PV = pore volume
R_{wa} = apparent water resistivityof a clean sandstone
T = temperature, °F
V_{disp} = volume dispersed clay
V_{sh} = volume of shale
V_{clay} = volume of clay
X = bulk volume fraction
γ = normalized gamma-ray scale using clean sand = 1 and shale = 0
ζ = parameter defined as $GR_{sh}/(GR_{sh} - GR_{sd})$
ϕ = porosity
ϕ_E = effective porosity
ϕ_T = total porosity

Subscripts

cl = clean sand
disp = dispersed shale
lam = laminated shale
sd = sand
sdgr = sand grains
shgr = shale grains
str = structural clay

REFERENCES

As I sat down to write references, I realized there were way too many to include them all; Stephen Prensky's Bibliography of Well-Log Applications does that for us. Thank you Steve. So I pared the list down the few I felt the readers could quickly assimilate and make use of in their daily tasks. Happy reading.

Hagiwara, T., 1988, Method for Analyzing Thinly Bedded Sand/Shale Formations, U.S. Patent No. 4,739,255, Published April 18, 1988.

Hill, H.J., and Milburn, J.D., 1956, Effect of Clay and Water Salinity on Electrochemical Behavior of Reservoir Rocks, Paper SPE-532-G (T.P. 4223), *Transactions, AIME Petroleum Branch*, **207**, 65–72.,

Klein, J.D., 1991, Induction Log Anisotropy Correction, Paper T, *Transactions, SPWLA 32nd Annual Logging Symposium*, Midland, Texas, USA, 16–19 June.

Lang, W.H., Jr., Brown, A.A., Berry, W.R., IV, Coates, G.R., Fertl, W.H., Hoyer, W.H., Patchett, J.G., and Ransom, R.C., editors, 1982, Shaly Sand, SPWLA Reprint Volume. Includes six chapters and a bibliography.

Prensky, S., 1987–2002, Bibliography of Well-Log Applications. Published annually in *The Log Analyst/Petrophysics*.

Thomas, E.C., and Haley, R.A., 1977, Log Derived Shale Distribution in Sandstone and its effect Upon Porosity, Water Saturation and Pemeability, Paper N, *Transactions, CWLS 6th Formation Evaluation Symposium*, Calgary, Alberta, Canada, 24–26 October.

Winsauer, W.O., and McCardell, W.M., 1953, Ionic Double-Layer Conductivity in Reservoir Rock, Paper T.P. 3565, *Transactions, AIME Petroleum Branch*, **198**, 129–134. Reprinted in 1982, SPWLA Shaly Sand Reprint Volume. III-121–III-126.

ABOUT THE AUTHOR

E.C. Thomas is a consulting petrophysicist and owner of Bayou Petrophysics and provides technical training in shaly sand analyses and all other areas of petrophysics for Petroskills. E.C.'s professional career interests and publications have spanned the entire field of formation evaluation/reservoir characterization, i.e., petrophysics. In 1992, he wrote a biographical sketch of Gus Archie for *The Log Analyst* to commemorate the 50th anniversary of the publication of the Archie Equation.

E.C. retired from Shell E&P Technology Company as a Petrophysical Advisor where he actively pursued research and field evaluation topics in the area of Petrophysics for over 32 years. He also authored and taught basic, intermediate and advanced courses in petrophysics for more than seven years at Shell's Training Center. E.C. 's academic background includes a BS in Chemistry from LSU, a PhD in Physical Chemistry from Stanford University, and a year of postdoctoral research in Physical Chemistry at Princeton University

E.C. has served SPWLA and SPE in many capacities, including SPE Distinguished Lecturer and chairman of the 1998 Archie Conference. Professional recognitions have included invitations to serve as keynote speaker at several SPE and SPWLA regional and topical conferences, and at the 2005 SPWLA Annual Symposium. In 2000, E.C. received the SPWLA Distinguished Technical Achievement Award; and in 2004, the SPWLA Gold Medal Award for Technical Achievement. E.C. served as a Petrophysical Consultant to the President's Commission investigating the BP-Deepwater Horizon blowout and resulting oil spill. E.C. currently serves as a technical reviewer for *Petrophysics* and *SPE Reservoir Evaluation & Engineering.*